

A new technique to provide realistic input to CME forecasting models

Nat Gopalswamy¹, Sachiko Akiyama², Seiji Yashiro², and Hong Xie²

¹ Solar Physics Laboratory, NASA Goddard Space Flight Center, Greenbelt, MD 20771, USA
email: nat.gopalswamy@nasa.gov

²Dept. of Physics, The Catholic University of America, Washington DC 20064, USA

Abstract. We report on a technique to construct a flux rope (FR) from eruption data at the Sun. The technique involves line-of-sight magnetic fields, post-eruption arcades in the corona, and white-light coronal mass ejections (CMEs) so that the FR geometric and magnetic properties can be fully defined in addition to the kinematic properties. We refer to this FR as FRED (Flux Rope from Eruption Data). We illustrate the FRED construction using the 2012 July 12 eruption and compare the coronal and interplanetary properties of the FR. The results indicate that the FRED input should help make realistic predictions of the components of the FR magnetic field in the heliosphere.

Keywords. coronal mass ejection, flux rope, reconnection.

1. Introduction

Coronal mass ejections (CMEs) are the most important players in space weather because they cause the severest of geomagnetic storms and accelerate energetic particles to GeV energies. The intensity of geomagnetic storms as measured by the Dst index primarily depends on the magnitude of the out-of-the-ecliptic (B_z) component of the interplanetary magnetic field and the speed (V) with which the structure impacts Earth's magnetosphere: $Dst = -0.01V|B_z| - 32$ nT (Wu & Lepping 2002; Gopalswamy et al. 2008). One of the vexing problems in space weather has been the prediction of the southward component (negative B_z) that reconnects with Earth's magnetic field to produce geomagnetic storms. While there has been reasonable progress in the prediction of the arrival time of CMEs, B_z prediction has been very limited due to the lack of realistic input to global MHD models that track CMEs into the heliosphere and provide asymptotic values of the CME parameters including the magnetic field. Since most CMEs arriving at Earth have a flux rope (FR) structure, it is inevitable that the global MHD models should use a FR input at the near-Sun boundary. Current models use a pressure pulse (which has no magnetic content) or ad hoc magnetic structures such as a spheromak (Odstrcil & Pizzo 1999; Jin et al. 2017; Shen et al. 2014; Shiota et al. 2014).

We construct a “flux rope from eruption data” (FRED) by combining two key results: (i) the reconnected (RC) flux during an eruption approximately equals the poloidal flux of the ejected flux rope (Longcope et al. 2007; Qiu et al. 2007; Hu et al. 2014; Gopalswamy et al. 2017a), and (ii) white-light or EUV coronal mass ejections (CMEs) can be fit to a FR to get its geometrical properties (see e.g., Temmer et al. 2011). The RC flux is computed from the area under post-eruption arcades and the underlying unsigned photospheric magnetic field strength. The poloidal flux of the FR is known from the RC flux; assuming that the FR is force free (Lundquist) we can get the axial and azimuthal field components and the toroidal flux of the flux rope. Thus we have a fully-defined FR, complete with geometric and magnetic parameters that can be input to global MHD

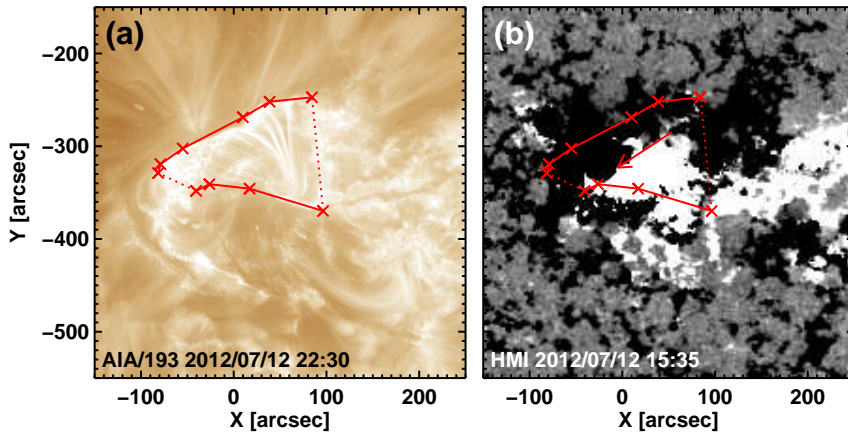


Figure 1. (a) PEA from SDO/AIA 193 Å with the area outlined by a polygon. (b) SDO/HMI magnetogram with PEA area and the direction of the filament magnetic field (arrow) overlaid.

models. The axial and poloidal fields are essentially responsible for geoeffectiveness in high and low-inclination magnetic clouds at Earth, respectively and hence the FR input should lead to definite prediction schemes. The FRED technique is complementary to another one that uses the source-region relative magnetic helicity along with FR geometrical properties to estimate the FR magnetic properties (Patsourakos et al. 2016).

2. The Coronal Flux Rope

We illustrate the construction of FRED using the 2012 July 12 eruption that resulted in an SEP event and a large geomagnetic storm. The event has been studied by many authors (see e.g., Gopalswamy et al. 2013; Gopalswamy et al. 2014; Hess & Zhang 2014; Möstl et al. 2014; Hu et al. 2016). Most of these papers were concerned with the kinematics and Sun-to-Earth propagation of the CME that ended up as a shock-driving magnetic cloud at Earth. Many of the authors also fit a flux rope using the graduated cylindrical shell (GCS) model (Thernisien 2011). Here we use the GCS model to get the geometric parameters of the FR.

Geometrical Properties. Fitting the CME observed by the three views provided by the SOHO and STEREO missions to the GCS model, we get the coordinates of the flux rope as S12W06, which is slightly different from the flare location in AR 11520 (S15W01, Gopalswamy et al. 2014). The ratio of the FR radius (R_0) to the leading edge distance from the Sun center (R_{tip}) is 0.26. At $R_{tip} = 10$ Rs, the $R_0 = 2.6$ Rs. The face-on and edge-on angular widths of the FR are 94 and 40 degrees, respectively. The tilt angle of the FR axis at its apex with respect to the horizontal is about 53 degrees, indicating a northwest-southeast orientation of the flux rope axis. neutral line and inferred from filament location.

Magnetic Properties. We combine these geometrical information with the RC flux to get the magnetic properties of the FR. It was recently shown that the total RC flux during an eruption can be obtained from a snapshot of the post eruption arcade (PEA) and the underlying photospheric magnetic field (Gopalswamy et al. 2017a). Fig. 1 shows a snapshot of the PEA associated with the 2012 July 12 eruption as observed by the Atmospheric Imaging Assembly (AIA) on board the Solar Dynamics Observatory (SDO) at 193 Å. Also shown is the corresponding photospheric magnetic field from SDOs He-

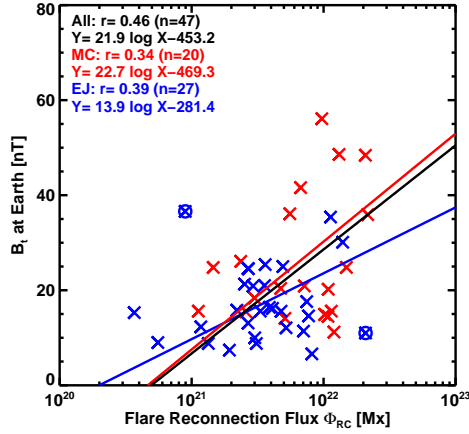


Figure 2. Scatter plot between observed B_{tot} and ϕ_r for a set of events from solar cycle 23 reported in Gopalswamy et al. (2017b). Two outliers are excluded from the correlation. Blue and red symbols correspond to magnetic clouds (MC) and non-cloud ejects (EJ), respectively.

lioseismic and Magnetic Imager (HMI). The arrow in Fig. 1(b) points to the direction of the axial magnetic field of the erupted flux rope based on filament connectivity. The axis is tilted by about 46 degrees to the horizontal. The area of the polygon in Fig. 1(a) is $7.2 \times 10^{19} \text{ cm}^2$, and an average magnetic field strength of B of 392 G. The RC flux ϕ_r is thus $1.42 \times 10^{22} \text{ Mx}$, which is half the unsigned flux through the PEA area.

Since ϕ_r roughly equals the poloidal flux (ϕ_p) of the erupted FR, we can get the axial field (B_0) of the coronal FR from the relation, $\phi_p = (L/x_{01})B_0R_0$, where L is the FR length and x_{01} ($=2.4048$) is the first zero of the Bessel function J_0 . Taking $L = 2 R_{tip} = 20 R_s$, we get $B_0 = \phi_r x_{01}/LR_0 = 0.13 \text{ G}$, which is near the higher end of the axial field of coronal FRs reported in Gopalswamy et al. (2017b). The toroidal flux of the FR is $\phi_t = \phi_p(2\pi R_0/L)J_1(x_{01})$, where J_1 is the first order Bessel function. With the above numbers from the GCS fit, we get $\phi_t = 0.42\phi_p$ or $5.96 \times 10^{21} \text{ Mx}$. The poloidal (B_p) and toroidal (B_t) field strengths at any distance r from the FR axis are given by $B_p = HB_0J_1(\alpha r)$ with $H = \pm 1$ (helicity sign) and $B_t = B_0J_0(\alpha r)$. Here, $\alpha = x_{01}/R_0$ is the force-free parameter. In the present case, $H = +1$ because the axial field points mostly to the south and the azimuthal field goes from the positive to the negative side (see Fig. 1b). The direction is consistent with a southern hemispheric eruption having right-handed helicity sign (e.g., Bothmer & Schwenn 1998). Finally, the relative helicity per unit length (H_r/L) is also well-defined for a Lundquist FR: $H_r/L = 0.7B_0^2R_0^3$ (e.g., Dasso et al. 2003). For the 2012 July 12 coronal FR, $H_r = 9.98 \times 10^{43} \text{ Mx}^2$, if we take the FR length to be $2R_{tip}$. Thus, the flux rope is fully defined both geometrically and magnetically. The CME space speed was measured using STEREO-B as $V = 1548 \text{ km s}^{-1}$ (Gopalswamy et al. 2013). According to the empirical relation $V = 298\phi_r^{0.75}$ (Gopalswamy et al. 2017b), this speed indicates a ϕ_r of $9.0 \times 10^{21} \text{ Mx}$, which is about 36% smaller than the observed value ($1.42 \times 10^{22} \text{ Mx}$).

3. Comparison with 1-AU Observations

A recent study showed that the axial field of the coronal FR derived from $\phi-r$ correlates with the axial field of the 1-AU flux rope (fitted) and also with the strength of the observed total magnetic field (B_{tot}) (Gopalswamy et al. 2017b). Fig.2 shows a scatter

plot between ϕ_r and B_{tot} for a set of events from cycle 23. From the regression line $B_{tot} = 21.9\log\phi_r - 453.2$ nT, we get $B_{tot} = 31.9$ nT with $\phi_r = 1.42 \times 10^{22}$ Mx for the 2012 July 12 eruption. The inferred B_{tot} is very close to the observed value at 1 AU: ~ 30 nT (see e.g. Hess and Zhang 2014). If the FR expanded self-similarly, the 1-AU FR radius is expected to be 0.26 AU (since $R_0/R_{tip} = 0.26$ with $R_{tip} = 1$ AU). Therefore, can get the 1-AU axial field strength from the coronal field strength ($B_0 = 0.13$ G) as: $B_{01AU} = B_0(10/214)^2 = 28.3$ nT, again very similar to the observed value. The assumption of self-similar expansion seems to be valid because the FR radius is consistent with that obtained from Grad-Shafranov reconstruction using *in-situ* data (Hu et al. 2016). For the same reasons, H_r at 1 AU is similar to that in the coronal FR. The 1-AU data also shows that the flux rope rotates from west to east, while the axis points southward throughout the cloud duration (Hess & Zhang 2014; Hu et al. 2016), consistent with the orientation of the coronal FR. In this event, the B_z is simply the axial field component.

4. Discussion and Summary

FRED is shown to be a viable starting point to infer the expected asymptotic magnetic structure in the heliosphere. It combines the line of sight magnetograms and PEA observations (X-ray, EUV, H-alpha, or microwave) with CME observations in the corona to obtain the complete properties of coronal FRs. We have used a distance of 10 Rs for the purpose of illustration, but FRED properties can be obtained at any initial height where the CME is observed. Global MHD models that use a realistic input such as FRED should be able to provide a realistic forecast of what to expect in the heliosphere. It must be noted that additional effects such as CME deflection and rotation can modify the FR, which can be accounted for using semi-analytic models (see e.g., Kay et al. 2015).

Acknowledgement. Work supported by NASA Heliophysics GI and LWS programs.

References

- Bothmer, V., & Schwenn, R. 1998, *Annales Geophysicae*, 16, 1
- Dasso, S., Mandrini, C. H., Démoulin, P., & Farrugia, C. J. 2003, *JGR*, 108, 1362
- Gopalswamy, N., Xie, H., Akiyama, S., Mäkelä, P. A., & Yashiro, S. 2014, *Earth, Planets, and Space*, 66, 104
- Gopalswamy, N., Mäkelä, P., Xie, H., & Yashiro, S. 2013, *Space Weather*, 11, 661
- Gopalswamy, N., Akiyama, S., Yashiro, S., Michalek, G., & Lepping, R. 2008, *JASTP*, 70, 245
- Gopalswamy, N., Yashiro, S., Akiyama, S., & Xie, H. 2017, *SolPhys*, 292, 65
- Gopalswamy, N., Akiyama, S., Yashiro, S., & Xie, H. 2017, arXiv:1705.08912
- Hess, P., & Zhang, J. 2014, *ApJ*, 792, 49
- Hu, Q., Qiu, J., Dasgupta, B., Khare, A., & Webb, G. M. 2014, *ApJ*, 793, 53
- Hu, H., Liu, Y. D., Wang, R., Möstl, C., & Yang, Z. 2016, *ApJ*, 829, 97
- Jin, M., Manchester, W. B., van der Holst, B., et al. 2017, *ApJ*, 834, 173
- Kay, C., Opher, M., & Evans, R. M. 2015, *ApJ*, 805, 168
- Longcope, D., Beveridge, C., Qiu, J., et al. 2007, *SolPhys*, 244, 45
- Möstl, C., Amla, K., Hall, J. R., et al. 2014, *ApJ*, 787, 119
- Odstrčil, D., & Pizzo, V. J. 1999, *JGR*, 104, 483
- Patsourakos, S., Georgoulis, M. K., Vourlidas, A., et al. 2016, *ApJ*, 817, 14
- Qiu, J., Hu, Q., Howard, T. A., & Yurchyshyn, V. B. 2007, *ApJ*, 659, 758
- Shen, F., Shen, C., Zhang, J., et al. 2014, *JGR*, 119, 7128
- Shiota, D., Kataoka, R., Miyoshi, Y., et al. 2014, *Space Weather*, 12, 187
- Temmer, M., Veronig, A. M., Gopalswamy, N., & Yashiro, S. 2011, *SolPhys*, 273, 421
- Thernisien, A. 2011, *ApJS*, 194, 33
- Wu, C.-C., & Lepping, R. P. 2002, *JGR*, 107, 1346